JOURNAL OF APPLIED PHYSICS VOLUME 93, NUMBER 2 15 JANUARY 2003

Magnetization switching in 70-nm-wide pseudo-spin-valve nanoelements

Xiaobin Zhu^{a)} and P. Grütter

Department of Physics, Center for the Physics of Materials, McGill University, 3600 University Street, Montréal, Québec H3A 2T8, Canada

Y. Hao, F. J. Castaño, S. Haratani, and C. A. Ross

Department of Material Science and Engineering, Massachusetts Institute of Technology, Cambridge, Massachusetts 02139

B. Vögeli and H. I. Smith

Department of Electrical Engineering and Computer Science, Massachusetts Institute of Technology, Cambridge, Massachusetts 02139

(Received 14 August 2002; accepted 29 October 2002)

The magnetic domain structures and magnetization reversal of patterned 70-nm-wide pseudo-spin-valve (PSV) elements were studied by magnetic force microscopy (MFM). Both magnetically soft and hard layers form single-domain states at remanence, and can be magnetized either parallel or antiparallel to each other. The switching field of each layer, and the coupling between the layers, are quantified using MFM. Individual elements show well-defined switching fields, while the ensemble has a large switching field distribution due to variability between the PSV elements. © 2003 American Institute of Physics. [DOI: 10.1063/1.1531229]

I. INTRODUCTION

Lithographically patterned magnetic multilayer elements, such as magnetic tunneling junction (MTJ) (Ref. 1) and pseudo-spin-valve (PSV) elements,² are the key components in high density magnetoresistive random access memory (MRAM) devices.³ Recent studies have focused on examining the behavior of elements with submicron or deepsubmicron dimensions.^{4,5} These PSV or MTJ elements consist of asymmetric sandwiches containing two magnetic layers with different switching fields: one is magnetically soft and the other is magnetically hard. For elements with micron-scale dimensions, interactions between the layers can lead to their demagnetization,6 and complex domain structures such as unfavorable 360° domain walls can be formed. In comparison, the magnetic layers in elongated elements of sub-100-nm dimensions can show single-domain behavior. The switching process is abrupt and the layers will not be demagnetized by each other's fringe fields. Magnetoresistive (MR) behavior has been characterized for individual elements in both the current-in-plane (CIP) (Ref. 4) and currentperpendicular-to-the-plane (CPP) configurations.^{5,8} The elements can be reversed by applying a magnetic field, or by polarized current-induced switching.^{5,8} Sudden jumps in resistance corresponding to the switching of the magnetic layers have been clearly demonstrated. However, to date there has not been a study of the reversal of such small elements using magnetic force microscopy (MFM), or an investigation of their remanent states. In this work, we use high sensitivity, high resolution MFM with in situ applied magnetic fields to characterize the magnetic domain structures in such arrays and the switching behavior of single elements.

II. EXPERIMENTAL TECHNIQUES

The sample used in this study is an array of NiFe/Cu/Co/Cu PSV elements prepared using interference lithography (IL) and ion milling. The PSV film is a sandwich containing a hard magnetic layer and a soft layer (Co and NiFe, respectively, in this case) separated by a spacer layer. The individual elements have dimensions of 70 nm×550 nm, with NiFe, Cu spacer, and Co thicknesses of 6, 3, and 4 nm, respectively. Figure 1(a) shows a scanning electron microscope (SEM) image of the array. The magnetization behavior was previously studied by alternating gradient magnetometery (AGM), which gives the collective hysteresis loop of the array.

In the present study, the magnetic structures and magnetization reversal were studied using a custom-built vacuum MFM.¹¹ The magnetic probes used are silicon cantilevers sputter coated with 25 nm of a CoPtCr alloy. Two types of cantilevers were used: one with a resonance frequency of 68 kHz and spring constant of 1.5 N/m, and the second with corresponding parameters of 60 kHz and 0.9 N/m. To minimize the MFM tip-induced magnetic distortion, all MFM images were taken in constant height mode by allowing the MFM tip to fly above the sample plane at a user-controlled height, without tracking the sample topography. 12 By operating under moderate vacuum (1.0×10^{-5} Torr) and using a digital phase-locked loop to detect the cantilever frequency shift, 13 the minimum detectable force gradient in this system can be as small as 2×10^{-6} N/m with a cantilever oscillation amplitude of 15 nm. The images were taken at remanence to reduce the combined perturbing effects of the MFM tip and external field. The magnetic fields were applied in plane along the long axis of the elements, which is the easy axis due to shape anisotropy.

a) Electronic mail: xbzhu@physics.mcgill.ca

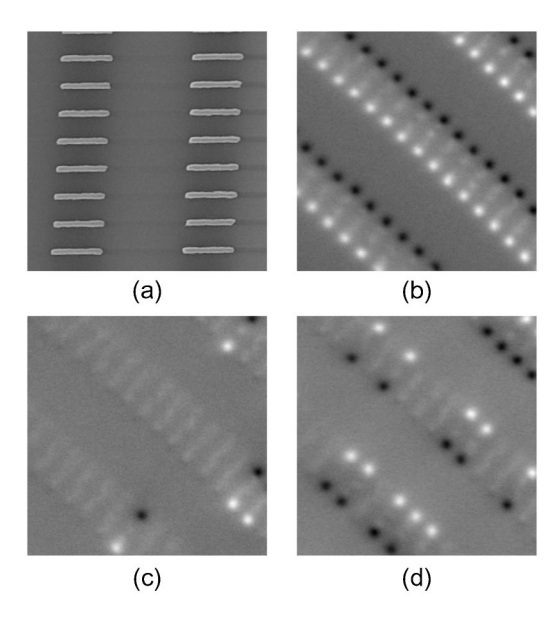


FIG. 1. (a) SEM image of the elements; MFM images taken at remanence: (b) after saturation at 800 Oe; (c) after subsequently applying -97 Oe; and (d) after subsequently applying -485 Oe. The gray scale corresponds to $\approx 1.7~{\rm Hz} \approx 5 \times 10^{-5}~{\rm N/m}$ force gradient.

III. RESULTS AND DISCUSSION

Figures 1(b)-1(d) show sequential images of the PSV structures after applying different fields. The remanent state, after saturation at 800 Oe [Fig. 1(b)], shows bright and dark contrast close to the element ends. This is a result of both magnetic layers having the same magnetization direction (the parallel or P state). However, if a magnetic field is then applied in the opposite direction, the magnetic moment in the soft (NiFe) layer can be switched to be antiparallel to the moment in the Co layer. This is described as an AP state. The observed magnetic contrast is very weak because the stray fields of the NiFe and Co layers almost exactly cancel each other for the layer thicknesses used here. As the opposite field is increased, more of the low moment AP states are formed, as shown in Fig. 1(c). Above a critical field, all element are in the AP state. If the magnetic field is increased further, the magnetic moment in the hard (Co) layer is reversed and a P state is formed that is oriented opposite to the original P state, as shown in Fig. 1(d).

By performing large-area scans with an external field, the remanent MFM "hysteresis loop" can be obtained, ¹⁴ as shown in Fig. 2. The solid dots show the combined remanent hysteresis loop of 460 ± 10 elements. The broad switching field distribution is a result of different individual elements having different switching fields. The moment in the soft NiFe layer reverses at a small field, labeled H_{c1} , which averages approximately 80 Oe, though some elements reverse at 25 Oe and others at 125 Oe. The switching field range is thus at least 100 Oe. An even wider variation (400 Oe) is found for the hard layer switching field H_{c2} . H_{c2} averages 480 Oe, though reversal occurs at fields between 300 and 700 Oe.

However, for an individual element, we find square hysteresis loops with abrupt switching at well-defined field values of H_{c1} and H_{c2} . The magnetization reversal of indi-

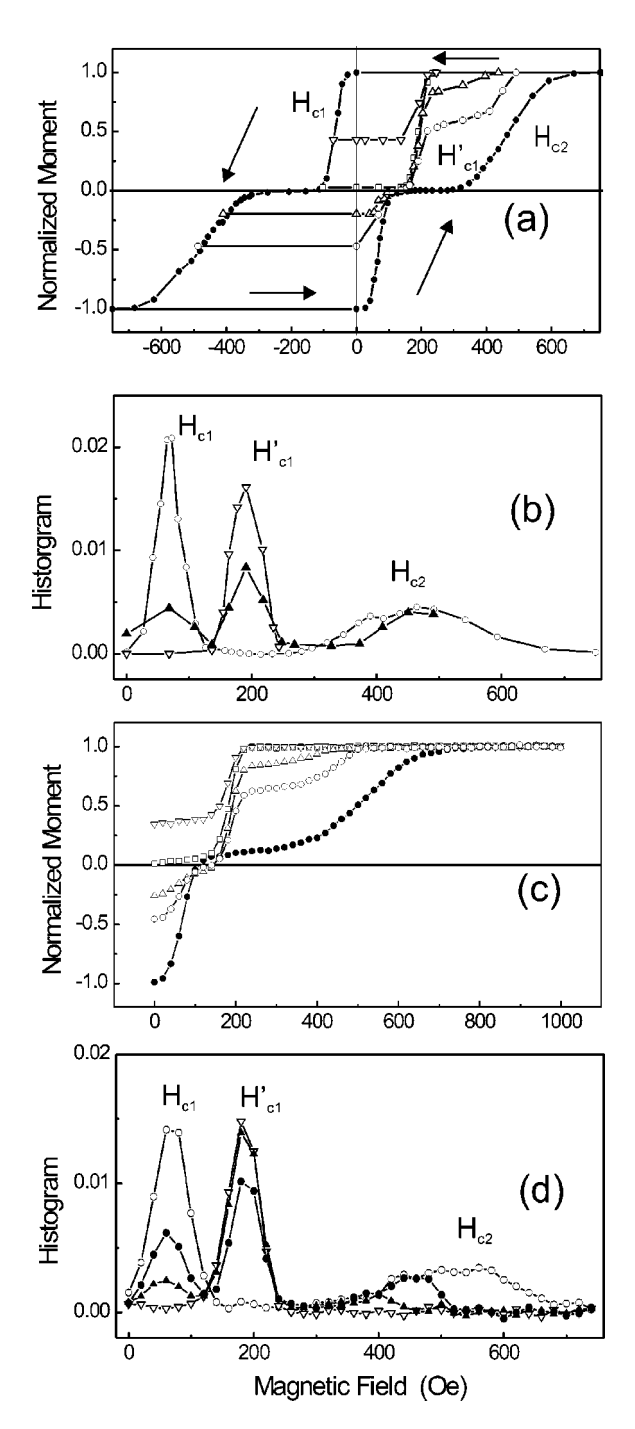


FIG. 2. (a) Major (solid dots) and minor remanent hysteresis loops obtained by MFM; open dots: minor loop with a starting field of -488 Oe; up triangle: -410 Oe; square: -102 Oe; and down triangle: -70 Oe. The major loop is based on measuring 460 elements, the minor loops on 170 elements; (b) differential curve of (a) for the major loop (open dots) and the minor loops with starting fields of -102 Oe (down triangle) and -488 Oe (up triangle); (c) Half of major and minor remanent loops of 10⁹ elements measured using AGM; symbols represent the same starting fields as those in (a); (d) differential curve of the AGM remanent major and minor hysteresis loops; circular open dot: major loop; solid dot: minor loop with a starting field of -488 Oe; solid up triangle -410 Oe; and open down triangle dot -102 Oe. Dots are connected for clarity.

vidual elements may be studied by imaging the element at different fields, but it is more convenient to measure a local hysteresis loop without scanning. ¹⁵ As shown in the inset of Fig. 3(a), to perform this measurement the MFM tip is lo-

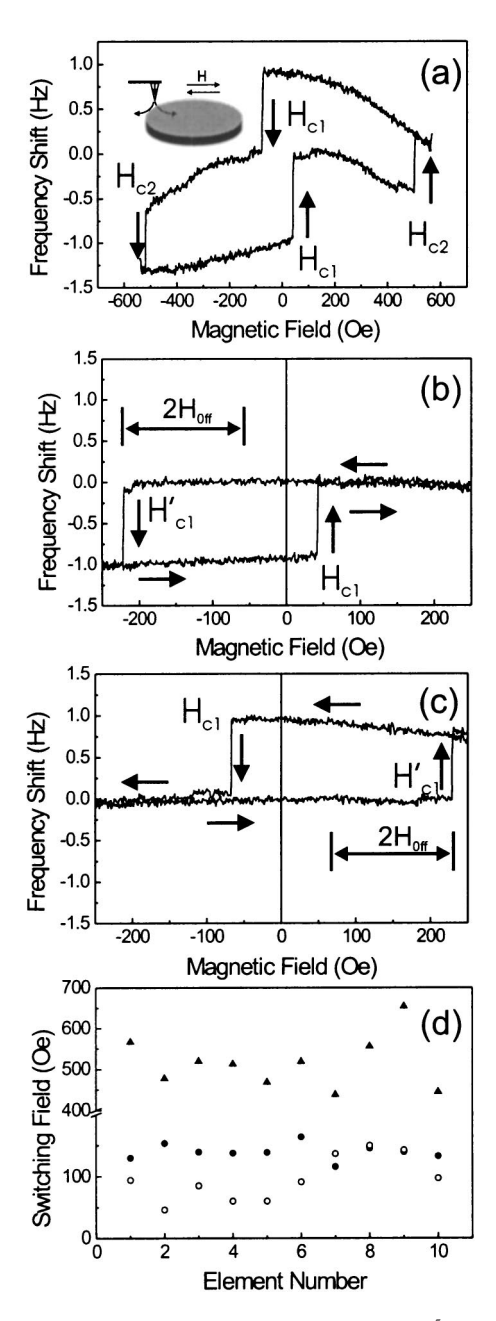


FIG. 3. Hysteresis loop of a single element. 1 Hz \approx 3×10⁻⁵ N/m, (a) major loop; (b) minor loop starting from the *P* state, (c) minor loop starting from the opposite *P* state. The MFM tip was located at one end of the element as shown in the inset of (a). The large difference between H_{c1} and H'_{c1} is caused by the interaction with the hard layer. (d) switching field distribution of H_s (solid circular dots), H_{c2} (solid up triangles) and offset field $H_{\rm off}$ (open circular dots) for ten different individual elements.

cated at one end of an element, and the cantilever frequency shit is monitored while sweeping the external field. The cantilever frequency shift is proportional to the force gradient between the tip and the sample. The observed frequency shift is thus a measure of the local sample moment. Figure 3(a) shows the hysteresis loop of a selected dot. Two distinct frequency changes are clearly visible at applied fields H_{c1} and H_{c2} , which correspond to the soft layer (H_{c1}) and the hard layer (H_{c2}) switching. The abrupt frequency changes, and the images in Fig. 1, suggest that both the soft and hard layers switch between two oppositely oriented single-domain

states. However, we cannot necessarily conclude that the switching process is classical coherent rotation, as end domain structures may be trapped at the edges of the elements.

Minor loops of a single element were measured by sweeping the external field between $\pm H$ where $H_{c1} < H$ $< H_{c2}$. In this case, only the soft layer is switched and the element cycles between the P and the AP states. Typical examples are shown in Figs. 3(b) and 3(c). A large field of 800 Oe (-800 Oe) was first applied to saturate both layers to form a P state, and then an opposite field was ramped to -H(H) to form the AP state. However, if the field is then ramped backward to H(-H) as indicated by the arrows in Fig. 3(b) [Fig. 3(c)], the soft magnetic layer is switched back to form the P state at a field $H'_{c1}(-H'_{c1})$, which is larger than H_{c1} , but much smaller than H_{c2} . The asymmetric switching of the minor loop is due to the magnetic coupling between the two magnetic layers, as a result of magnetostatic interactions and of exchange coupling through the 3 nm Cu layer spacer. It is worth pointing out that Figs. 3(b) and 3(c) are realistic hysteresis loops of a PSV element when it is used in a MRAM cell. The observation is that the loop is nearly a perfect square in shape with sharp magnetization transitions.

We can express the magnetic coupling between the two layers as an offset field $H_{\rm off}$, which the hard layer exerts on the soft layer. This field is indicated in Figs. 3(b) and 3(c). The switching field for an isolated soft layer, in the absence of the hard layer, will be $H_s = (H_{c1} + H_{c1}')/2$, while $H_{\rm off} = (H_{c1}' - H_{c1})/2$. We found that for any particular element switching and offset fields are very reproducible, with variation less than 10 Oe between measurements. However, the switching and offset fields show considerable variation from element to element. Figure 3(d) shows a plot of H_s , $H_{\rm off}$, and H_{c2} for ten different elements. The offset field has substantially larger variability than the soft layer switching field.

Minor loops of the array were studied by acquiring MFM images after applying different fields. Figure 2(a) additionally shows four remanent minor loops at starting fields of -70, -102, -410, and -488 Oe, measured for 170 ± 5 elements. It is convenient to describe the four possible magnetization states that can coexist in the array as A, B, C, and D as shown in Fig. 4, where A and B are the two possible Pstates and C and D are the two AP states. Upon positive saturation, all elements are in the B state. In the minor loops corresponding to small reverse fields (-70 and -102 Oe), most elements remain in the initial B state and only a small percentage of the elements are switched from the B state to the D state by the reverse field. As the field is ramped back towards positive saturation, the soft layer in the D state is switched back to recreate the B state at a field H'_{c1} . However, when compared to Fig. 3(b), the minor loop is not a perfect square shape, since the abrupt transition of the individual elements in washed out by the switching field variation between the elements in the array. At larger reverse field (-410 and -488 Oe), the sample consists of a mixture of A and D states. We observe that three different switching processes appear as the field is ramped back to positive saturation. The elements in the A state are first switched to the C state at a field H_{c1} and then to the B state at a field H_{c2} . Elements in the D state are switched directly to the B state at

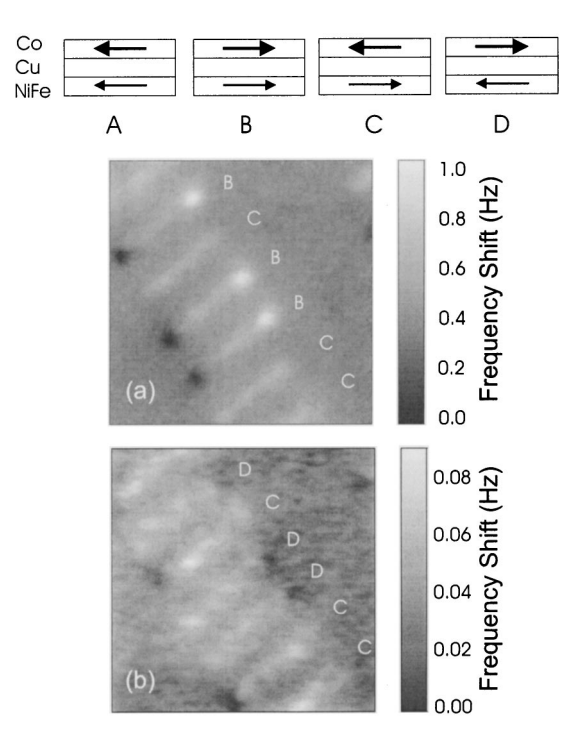


FIG. 4. Top: diagram of the four possible magnetic states in the PSV elements. (a) mixtures of antiparallel states and parallel states formed after applying 480 Oe reverse field to a previously saturated array; (b) coexistence of the two different antiparallel states, after subsequently applying a positive field of 135 Oe. 1 $Hz\approx4\times10^{-5}$ N/m.

a field H_{c1}' . This switching behavior can be clearly seen by constructing differential curves of Fig. 2(a). Figure 2(b) shows the differential curves for the major and minor loops at a starting field of -102 and -488 Oe. For the major loop, there are two distinct peaks at fields H_{c1} and H_{c2} , representing soft layer and hard layer switching. For the minor loop at -102 Oe, only one peak at field H_{c1}' is observed, which is associated with the switching from the D to the B state [see, also, Fig. 3(b) or 3(c)]. However, at a field of -488 Oe, 41% of the elements are switched to the A state, while the others are in the D state, and the differentiated minor loop shows three distinct peaks at fields H_{c1} , H_{c1}' , and H_{c2} . Figures 2(c) and 2(d) show the corresponding data acquired by AGM on a sample with 10^9 elements. There is excellent agreement between the AGM and MFM data.

So far, by assuming that both the Co and NiFe layers are single-domain elements, which can adopt P or AP configurations, we can successfully explain our experimental observations. In the following, we will show that highly sensitive MFM can be used to visualize distinctly the AP states as well as the P states. A field of -800 Oe was first applied to form the A state. Figure 4(a) shows the MFM image of the sample after applying 480 Oe reverse field. Some elements were switched to the B state, while the others formed the C state. If the field is then switched back to a value in between H_{c1} and H'_{c1} , for instance, 135 Oe, the C states remain, while the elements in B states are changed to D states. Figure 4(b) clearly shows the C and D antiparallel states coexisting. The gray scale contrast in this image is only about 0.09 Hz, which is about 10% of the value obtained for the parallel state image. The result is in good agreement with the relative magnetizations of the parallel and antiparallel states obtained by AGM. The signal is so small that some unavoidable topographic contrast also appears in the images. The low magnetic contrast occurs because the two magnetic layers form a closed flux loop with very small external stray field. Better contrast can be achieved by increasing the MFM tip moment, but this can perturb the magnetic states of the elements. The observed *P* or AP states are consistent with the remanent states of individual elements calculated using a micromagnetic simulation. ¹⁸ The AP state is very stable and consists of two single-domain layers antiparallel to each other, while in the *P* state, the moments in each layer are parallel to each other but show a small curling of the magnetization at the edges due to the strong demagnetizing field.

It is critical to maintain a narrow switching field distribution if PSV elements are to be used in MRAM. During cycling of the soft layer, the switching field distributions for $-H_{c1}$ and H_{c1}' should not overlap, and neither should the distributions of $-H_{c1}$ and $-H_{c2}$, to avoid inadvertent writing of elements during the readback process. MFM analysis has indicated that there are no overlaps in the array studied here, because the Co layers have relatively large switching fields compared to the NiFe layers. However, it is desirable to reduce the switching field distributions so that a lower hard layer switching field, and therefore a lower write current, can be tolerated.

In order to achieve this, the origins of the switching field distribution need to be understood. It may seem unexpected that nominally identical elements should show a wide range in switching behavior. However, this is a common observation for a variety of lithographically patterned structures, for example, in cylindrical or prismatic particles. $^{19-21}$ Although the elements appear to be identical, they have differences in edge roughness and microstructure. Magnetic reversal is often nucleated at such imperfections, so that even modest variability in microstructure or roughness can cause a wide range in the switching field. Additionally, in multilayer elements such as the ones measured here, variation in interlayer coupling field $H_{\rm off}$ also increases the distribution of switching fields because $H_{\rm off}$ contributes to the effective field acting on the hard and soft layers during reversal.

Perhaps surprisingly, we found that $H_{\rm off}$ has a larger variation than soft layer switching field H_s , and the two do not appear to be correlated [Fig. 3(d)]. H_{off} is a result of coupling between the two layers, and is expected to be independent of the switching fields of the layers. There are two contributions to $H_{\rm off}$: magnetostatic interactions between the two layers, which depend on saturation moment, layer geometry, and film thickness, and therefore have some dependence on edge roughness; and exchange coupling through the Cu layer. Exchange coupling is sensitive to pinholes in the Cu layer and thickness variations, and it will also be affected by edge roughness and by intermixing of the layers at the edges of the elements, caused by the ion-milling etch process. Determining which of these factors are the major contributors to the variability in switching and offset fields, while difficult, is the key to the successful development of magnetoelectronic devices.

In summary, the collective and individual magnetization reversal of 70-nm-wide PSV elements has been studied using high sensitivity MFM with an *in situ* magnetic field. Our results indicate that the two magnetic layers can form either parallel or antiparallel magnetic configurations. Individual elements show abrupt switching behavior, with ideal, square-shaped hysteresis loops, but there is a spread in both the switching fields and in the interlayer coupling field between individual elements. This distribution may be a result of variability in shape or microstructure of the magnetic layers, or the roughness of the Cu spacer layer. Controlling the element shape and microstructure will help elucidate this problem.

ACKNOWLEDGMENTS

The work at McGill was supported by NSERC and FCAR. The work at MIT was supported by TDK and DARPA.

- ¹S. S. P. Parkin, K. P. Roche, M. G. Samant, P. M. Rice, R. B. Beyers, R. E. Scheuerlein, E. J. O'Sullivan, S. L. Brown, J. Bucchigano, D. W. Abraham, Yu Lu, M. Rooks, P. L. Trouilloud, R. A. Wanner, and W. J. Gallagher, J. Appl. Phys. 85, 5828 (1999).
- ²B. A. Everitt, A. V. Pohm, R. S. Beech, A. Fink, and J. M. Daughton, IEEE Trans. Magn. **34**, 1060 (1998).
- ³J. M. Daughton, J. Magn. Magn. Mater. **192**, 334 (1999).
- ⁴L. Kong, Q. Pan, B. Cui, M. Li, and S. Y. Chou, J. Appl. Phys. **85**, 5492 (1999).
- ⁵F. J. Albert, J. A. Katine, R. A. Buhrman, and D. C. Ralph, Appl. Phys. Lett. **77**, 3809 (2000).

- ⁶M. R. McCartney, R. E. Dunin-Borkowski, M. R. Scheinfein, D. J. Smith, S. Gider, and S. S. P. Parkin, Science 286, 1337 (1999).
- ⁷X. Portier and A. K. Petford-Long, Appl. Phys. Lett. **76**, 754 (2000).
- ⁸J. A. Katine, F. J. Albert, R. A. Buhrman, E. B. Myers, and D. C. Ralph, Phys. Rev. Lett. **84**, 3149 (2000).
- ⁹F. J. Castano, Y. Hao, M. Hwang, C. A. Ross, B. Vogeli, H. I. Smith, and S. Haratani, Appl. Phys. Lett. **79**, 1504 (2001).
- ¹⁰ F. J. Castano, Y. Hao, C. A. Ross, B. Vogeli, H. I. Smith, and S. Haratani, J. Appl. Phys. **91**, 7317 (2002).
- ¹¹ P. Grütter, Y. Liu, P. LeBlanc, and U. Dürig, Appl. Phys. Lett. **71**, 279 (1997).
- ¹² X. Zhu, P. Grütter, V. Metlushko, and B. Ilic, J. Appl. Phys. **91**, 7340 (2002).
- ¹³ Digital PLL from Nanosurf AG, Liestal, CH.
- ¹⁴ We assign +1 or -1 to elements in the P state, and 0 to elements in the AP state, since the magnetization of the two layers in the AP state almost cancel each other.
- ¹⁵ X. Zhu, P. Grütter, V. Metlushko, and B. Ilic, Appl. Phys. Lett. **80**, 4789 (2002).
- ¹⁶The monotonic change in the cantilever frequency at large applied magnetic fields is caused by the stray gradient of the in-plane magnets.
- $^{17} {\rm The}$ free layer switching field is $H_{c1}^{\prime} H_{\rm off}$ or $H_{c1} + H_{\rm off}$.
- ¹⁸A public code from NIST. http://math.nist.gov/oommf. We use the 3D code Oxsii 1.2.
- ¹⁹C. A. Ross, M. Hwang, M. Shima, J. Y. Cheng, M. Farhoud, T. A. Savas, H. I. Smith, W. Schwarzacher, F. M. Ross, F. B. Humphrey, and M. Redjdal, Phys. Rev. B 65, 144417 (2002).
- ²⁰C. Haginoya, S. Heike, M. Ishibashi, K. Nakamura, K. Koike, T. Yoshimura, J. Yamamoto, and Y. Hirayama, J. Appl. Phys. 85, 8327 (1999)
- ²¹G. M. McClelland, M. W. Hart, C. T. Rettner, M. E. Best, K. R. Carter, and B. D. Terris, Appl. Phys. Lett. 81, 1483 (2002).